Preprints of the Fifth IFAC
Symposium on Robot Control
September 3-5, 1997, Nantes, France

Scale-Dependent Enveloping Grasps
— Inspired by Human Grasping —

Makoto Kaneko and Toshio Tsuji

Industrial and Systems Engineering, Hiroshima University
Higashi-Hiroshima, 739, JAPAN
E-mail: kaneko@huis.hiroshima-u.ac.jp, tsuji@huis.hiroshima-u.ac.jp

Abstract: This paper discusses the scale-dependent enveloping grasp. Human unconsciously changes the grasp strategy according to the size of objects, even though they have similar geometry. In wrapping a cylindrical object placed on a table, the grasping process by human can be roughly classified into three patterns according to the object's size. For a large cylindrical object, human wraps it directly without any regrasping process. As the diameter decreases, human begins to use the slip between finger link and the object. For a further small diameter, human first picks it up by finger tips and then makes grasp transition from finger tip to wrapping. We extract the essential motions from human grasping by utilizing the idea of virtual finger. A practical procedure for achieving an enveloping grasp is also presented especially for the second grasp pattern that utilizes the slipping motion.

Key words: Enveloping Grasp, Power Grasp, Scale-Dependent Enveloping Grasp, Constant Torque Control.

1 Introduction

There have been a number of works concerning multi-fingered robot hands. Most of them address a finger tip grasp, where it is assumed that a part of inner link of finger never makes contact with the object. Enveloping grasp (or power grasp) provides another grasping style, where multiple contacts between one finger and the object are allowed. Such an enveloping grasp can support a large load in nature and is highly stable due to a large number of distributed contact points on the grasped object. While there are still many works discussing enveloping grasps, most of them deal with the grasping phase only, such as contact force analysis, robustness of grasping and contact position sensing. Suppose that human eventually achieves an enveloping grasp for an object placed on a table. Actually, such a situation is often observed in a practical environment, for example, in grasping a table knife, an ice pick, a hammer, a wrench, and so on. In many cases, the tool handle can be modeled as a cylindrical shape. This is why we focus on cylindrical object as the first example. For a cylindrical object having a sufficiently large diameter, human will wrap it directly without any regrasping process, since the table makes no interference with the finger links. As the diameter decreases, human begins to use the slip between finger link and the object. For a further small diameter, however, human can not wrap it directly since the table interferes with finger link. Under such a case, human first picks it up by finger tips and then achieves the target style through the phase transition from the finger tip to the wrapping. More complicated transition phases may be observed depending on the diameter of the cylinder and on the person-dependent choice of grasp planning. These examples suggest that human chooses the grasp planning according to the scale of objects, even though they are geometrically similar. We call the grasp planning the scale-dependent grasp planning. Although the series of human motion are so fast that we can not clearly decompose it into individual motions, for robot application, we extract the essential motions from human grasping by utilizing the idea of virtual finger.

In this paper, we are particularly interested in the slip-based grasp, where human utilizes the wedge effect by pushing each finger between the object and the table, so that a lifting force can be generated. A practical

procedure for achieving an enveloping grasp is also presented especially for the slip-based grasp.

2 Related Work

Human grasping based approach: In robotic hands, there have been a number of papers learnt by human behaviors[1]–[5]. Cutkosky and Wright[1] have analyzed manufacturing grips and correlation with the design of robotic hands by examining grasps used by humans working with tools and metal parts. They classified the human grasps into two big categories, one is emphasized on stability and security (power grasp) and the other on dexterity and sensitivity (precision grasp). Stansfield discussed the robotic grasping based on knowledge[4]. These works [1]–[4], and [5] focus on either the final grasp mode or finding an appropriate grasp posture under a set of grasp modes, target geometric characteristics and task description.

Jeannerod[6] has shown that during the approaching phase of grasping, the hand preshapes in order to prepare the shape matching with the object to be grasped. Bard and Troccaz[7] introduced such a preshaping motion into a robotic hand and proposed a system for preshaping a planar two-fingered hand by utilizing low-level visual data. Kaneko and Honkawa[8] proposed an active sensing method for localizing multiple contact points for an inner link based grasp.

Enveloping grasp or power grasp: Mirrza and Orin[9] applied a linear programming approach to formulate and solve the force distribution problem in power grasps, and showed a significant increase in the maximum weight handling capability for completely enveloping type power grasps. Trinkle[10] analyzed planning techniques for enveloping, and frictionless grasping. Salisbury[11] has proposed the Whole-Arm Manipulation (WAM) capable of treating a big and heavy object by using one arm which allows multiple contacts with an object. Bicchi[12] showed that internal forces in power grasps which allow inner link contacts can be decomposed into active and passive. Omata and Nagata[13] also analyzed the indeterminate grasp force by fixing their eyes upon that contact sliding directions are constrained in power grasps. Zhang et. al.[14] evaluated the robustness of power grasp by utilizing the virtual work rate for all virtual displacements. Kleinmann et.al.[15] showed a couple of approaches for finally achieving power grasp from finger tip grasp. In our previous work[16], we have shown a preliminary work on Scale-Dependent Grasp.

3 Observation of human behavior

A subject sitting on a chair is commanded in such a way that he grasps a cylindrical object placed on a table in finally a wrapping style. Each examinee executes eighteen trials for various cylindrical objects with eighteen different diameters D. Fig.1 shows the change of grasp strategy according to the diameter of cylinder, where the horizontal and vertical axes are the length L from

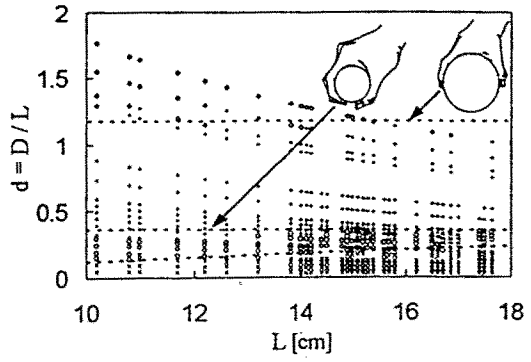

Fig.1 Grasp strategy classification map

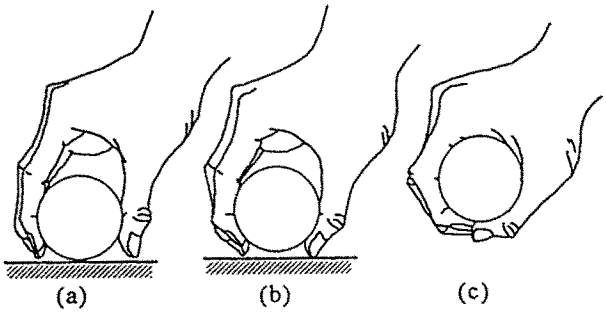

Fig.2 Two-VFs-based transition grasp

thumb's tip to pointer's tip and the normalized diameter of cylinder d given by $d = D/L$. The discussion utilizing d is very convenient since it is non-dimensional and, therefore, suppress the scale effect brought by the hand size. $\diamond$ denotes that a subject cannot grasp the object due to its large diameter, $+$ denotes that the person's hand wraps around it directly without any re-grasping process, $\circ$ denotes that the person first lifts the object from the table by utilizing a wedge effect between the fingers and the object, as shown in Fig.2(b), and then closes each finger around the object to achieve the target grasp (Fig.2(c)), and $\times$ denotes that the subject first picks up the object between his/her index finger and thumb, and then the remaining fingers hook the object and squeeze it till the finger tip grasp is broken and the object contacts the palm, as shown in Fig.3. Both the second and the last grasps are accompanied by grasp transition, such as that from finger tip to wrapping grasps. In both the first and the second grasps, the remaining fingers except thumb can be replaced by a virtual finger (VF), since they act as if they were just one finger. In the last grasp, the fingers other than the index finger and thumb can be regarded as a VF in the last grasp. Although there are, of course, some subjects utilizing exceptional grasp strategies, most of them exhibit a similar tendency to change the grasp strategy according to the size of object. If we remove the ungraspable region from Fig.1, the grasp strategies can be classified into three groups, direct grasp, Two VFs-based transition grasp, and Three VFs-based transition grasp, respectively.

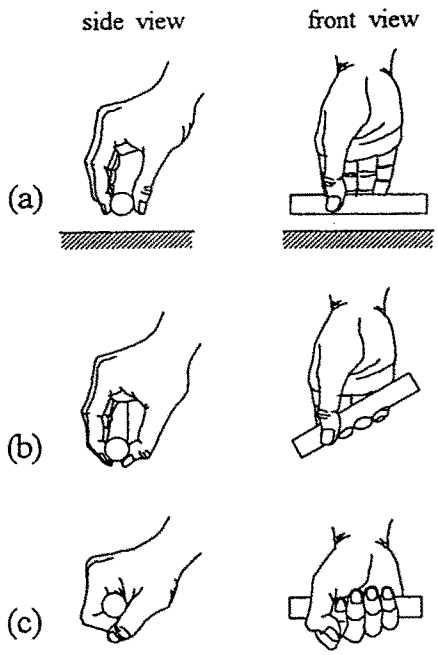

Fig.3 Three-VFs-based transition grasp

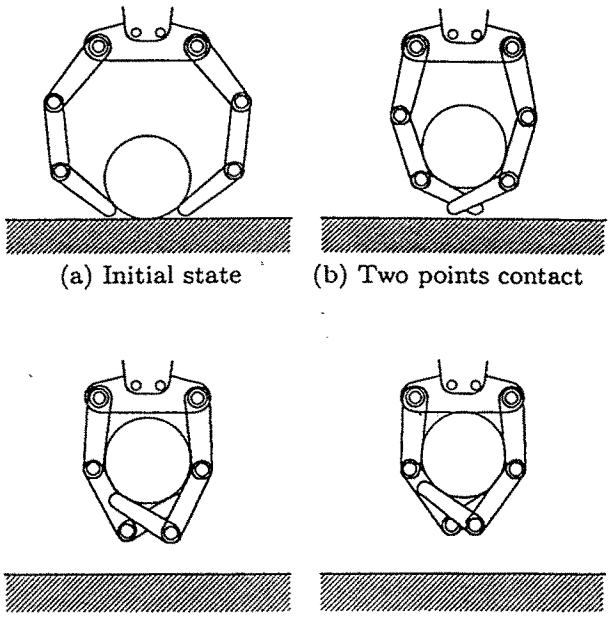

Fig.4 Two-VFs-based transition grasp

4 Scale-Dependent Grasp by Multi-Fingered Robot Hands

Since the direct grasp can be easily realized if a robot hand can satisfy the geometrical condition, we do not discuss this strategy here. Instead, focusing two other grasp strategies, we extract essential motions which are applicable for a robot hand. Also, to simplify the discussions, we assume that a three-fingered robot hand has three d.o.f for each finger and each link and the palm are of equal length, and that the robot knows the object shape and its position in advance.

A. Two VFs-Based Transition Grasp

As the diameter of the cylinder decreases, there exists a critical switching point where the direct wrapping can be realized any more since the table causes interference with the fingers. As mentioned before, the grasp strategy can be explained by two VFs as shown in Fig.4, where each finger tip makes contact with the object surface in Fig.4(a). In the next step, each finger tip pushes the object each other, so that we can make the most use of the wedge effect. Then, the object will be automatically lifted up by the slip between the finger tip and the object surface. Each finger link is closed to remove the degrees of freedom of the object gradually. By this motion, both the second and the third links will make contact with the object (two-points-contact mode), as shown in Fig.4(b). At this moment, the outputs from joint torque sensors abruptly increase, because the degree of freedom of finger along the table surface is no more available under such multiple contacts. By utilizing a large joint torque as a trigger signal, we switch to a constant torque control mode, in which a constant torque is commanded in each joint for finally making the object contact with the palm in addition to all links as shown in Fig.4(d). Whether the object really reaches the palm or not and how firmly grasp the object, strongly depend on how much torque command is imparted to each joint.

B. Three-VFs-based transition grasp

The Three-VFs-based transition grasp can be decomposed into two basic motions. One is the motion for picking up the object by using the index finger (finger 1) and thumb (finger 2) as shown in Fig.5(b), and the other is a series of motions for achieving the target grasp by using the last finger dexterously as shown in Fig.5(c)–(f). The first motion plays an important role in allowing no interference from the table, and can be easily realized if the object shape and location are perfectly given to the robot hand. In the following series of motions, the tip of the finger 3 first hooks the object and draws it toward the palm. By this finger motion, the object will rotate around the grasp axis formed by the fingers 1 and 2, unless the contact distance between the finger 3 and the finger 2 (or the finger 1) is too small. In order to realize the rotating slip, we can apply the existing approaches. After a part of object does make contact with the palm, we can regard the contact point between the palm and the object as a support point for a lever. Therefore, on increasing the drawing force, the finger tip grasping by the fingers 1 and 2 will eventually be broken for a large drawing force imparted by the finger 3(Fig.5(e)). By utilizing the inertia effect after breaking contact, the finger 3 can hold down the object against the palm. After that, both fingers 1 and 2

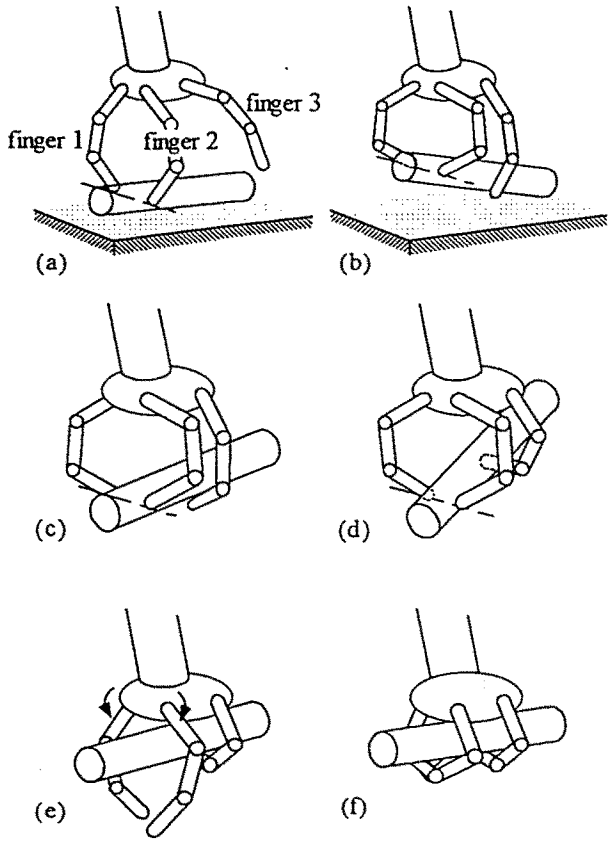

Fig.5 Three-VFs-based transition grasp

wrap the object quickly. This motion planning is simple enough so that we may be able to implement it to a multi-fingered robot hand, even though human being exhibits more complicated motion planning for such an object.

5 Analysis of Two-VFs-based transition grasp

For simplifying the discussions, we impart the following assumptions.

- Assumption-1: The robot hand has two fingers and each finger has two joints.
- Assumption-2: Each link always has one contact point.
- Assumption-3: The base distance and the link length have unit length.

Fig.6 shows the coordination and the definitions of notation for 2D cylindrical model, where R, $(x_G, y_G)^T$, $\tau=(\tau_{1,1}, \tau_{1,2}, \tau_{2,1}, \tau_{2,2})^T$ and $\theta_{i,j}$ denote the radius of the object, the position of the center of gravity of the object, the commanded torque, and the joint position with respect to the horizontal line. If R and $(x_G, y_G)^T$ are given, it is clear that the posture of the link is uniquely determined. As a result, the posture of the object and the link is a function of $(x_G, y_G)^T$ alone. Let

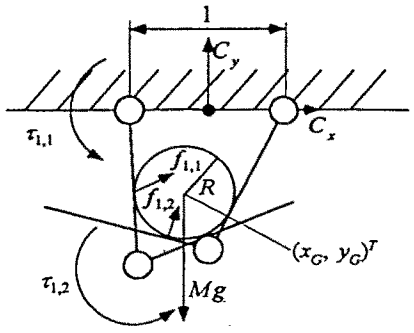

Fig.6 Definition of notation for 2D cylindrical model

$p_{i,j}=(p_{i,j,x}, p_{i,j,y})^T$ be a position vector of the contact point on the ith finger and jth link (i=1, 2, j=1, 2) and $e_{i,j}=(e_{i,j,x}, e_{i,j,y})^T$ be a position vector of the tip of each link, respectively. Since a contact force always appears within the friction cone, it can be represented by

$$f_{i,j} = \sum_{m=1}^{2} \lambda_{i,j}^m v_{i,j}^m \qquad (\lambda_{i,j}^m \geq 0) \tag{1}$$

$$= V_{i,j}\lambda_{i,j} \tag{2}$$

where $V_{i,j}$ is the unit vector directing the boundary of the friction cone, $V_{i,j} = [v_{i,j}^1, v_{i,j}^2]$ and $\lambda_{i,j} = [\lambda_{i,j}^1, \lambda_{i,j}^2]^T$. For two fingers, we have the following relationship.

$$\tau = J^T f \tag{3}$$

$$f = V\lambda \tag{4}$$

where

$$J^T = \begin{bmatrix} J_{1,1}^T & J_{1,2}^T & \mathbf{o} & \mathbf{o} \\ \mathbf{o} & \mathbf{o} & J_{2,1}^T & J_{2,2}^T \end{bmatrix} \tag{5}$$

$$J_{i,1}^T = \begin{bmatrix} e_{i,0,y} - p_{i,1,y} & -e_{i,0,x} + p_{i,1,x} \\ 0 & 0 \end{bmatrix} \tag{6}$$

$$J_{i,2}^T = \begin{bmatrix} e_{i,0,y} - p_{i,2,y} & -e_{i,0,x} + p_{i,2,x} \\ e_{i,1,y} - p_{i,2,y} & -e_{i,1,x} + p_{i,2,x} \end{bmatrix} \tag{7}$$

$$V = \begin{bmatrix} V_{1,1} & \mathbf{o} & \mathbf{o} & \mathbf{o} \\ \mathbf{o} & V_{1,2} & \mathbf{o} & \mathbf{o} \\ \mathbf{o} & \mathbf{o} & V_{2,1} & \mathbf{o} \\ \mathbf{o} & \mathbf{o} & \mathbf{o} & V_{2,2} \end{bmatrix} \tag{8}$$

$$V_{i,j} = \begin{bmatrix} -\sin(\theta_{i,j} - \alpha) & -\sin(\theta_{i,j} + \alpha) \\ \cos(\theta_{i,j} - \alpha) & \cos(\theta_{i,j} + \alpha) \end{bmatrix} \tag{9}$$

$$\lambda = \left[\lambda_{1,1}^T, \lambda_{1,2}^T, \lambda_{2,1}^T, \lambda_{2,2}^T\right]^T \tag{10}$$

The resultant force f_o is given by

$$f_o = \sum_{i=1}^{2}\sum_{j=1}^{2} f_{i,j} + Mg \tag{11}$$

$$= [V_{1,1}, \ldots, V_{2,2}]\lambda + Mg \tag{12}$$

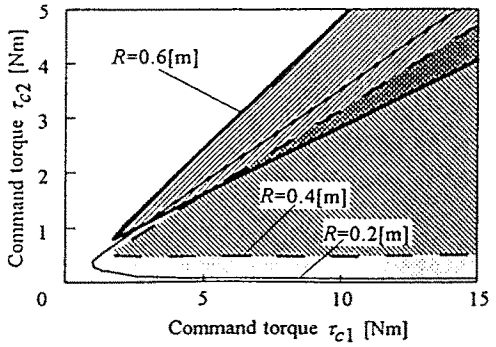

Fig.7 $\mathcal{T}$ in the constant torque command mode

Furthermore, we decompose the total force in the horizontal component f_h and the vertical component f_v as follows.

$$f_h = C_x^T f_o \quad (13)$$
$$f_v = C_y^T f_o \quad (14)$$

Under constant torque control, both f_h and f_v are bounded between the maximum and the minimum values of each axis of f_o. We can compute both the maximum and the minimum values by applying the linear programming problem given as follows.

Maximize or Minimize

$$f_h = C_x^T [V_{1,1}, \ldots, V_{2,2}]\lambda \quad (15)$$
or
$$f_v = C_y^T [V_{1,1}, \ldots, V_{2,2}]\lambda + Mg \quad (16)$$

Subject to

$$J^T V \lambda = \tau \quad (17)$$
$$\lambda_{i,j}^m \geq 0 \quad (18)$$
$$(i = 1,2,\ j = 1,2,\ m = 1,2)$$

Let f_v^+ and f_v^- be the maximum and minimum values of f_v, respectively. If $0 < f_v^- < f_v^+$ is satisfied, the object always receives the upward force, and a result, it starts to move toward the palm. On the other hand, if $f_v^- < f_v^+ < 0$ is satisfied, the object moves downward.

The hatched line in Fig.7 shows $\mathcal{T}$ computed for the hand in Fig.6, where $\mathcal{T}$ is defined such that the area ensures that the finger completely envelops the object until the object finally reaches the palm and mg is chosen by mg=1.0. From Fig.7, we can see a large area, while the area varies rather strongly depending upon the radius of the object. This radius dependency does not make much problem. Because the robot hand can roughly estimate the size of object by utilizing the link posture when a two-points contact is achieved. Therefore, we can choose the pair of τ_{c1} and τ_{c2} for the object whose radius is roughly given.

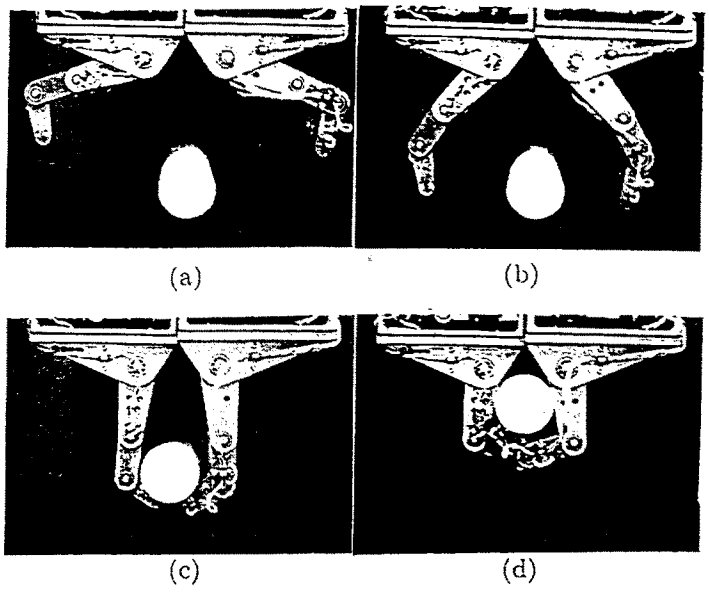

Fig.8 Grasping experiment (R=15[mm])

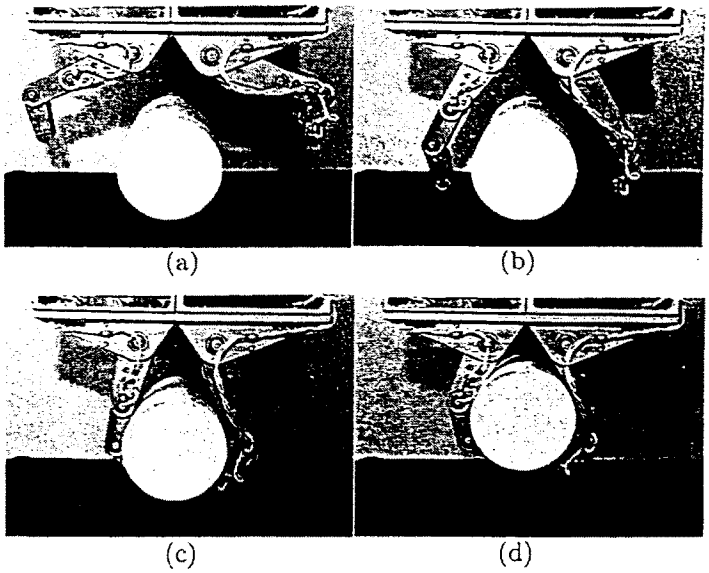

Fig.9 Grasping experiment (R=30[mm])

6 Experiments

Fig.8 shows continuous photos for a grasp experiment, where the radius of the object is R=15[mm]. The hand can complete the task very quickly, for example, the executing time for finally enveloping the object by the fingers was just 2.8 [sec]. Fig.9 also shows continuous photos for a different object whose radius is 30[mm]. Fig.10 shows the success and failure map (R=22.5[mm]) obtained by experiments when changing the commanded torque for each joint, where the black and the white symbols denote the success and the failure of enveloping

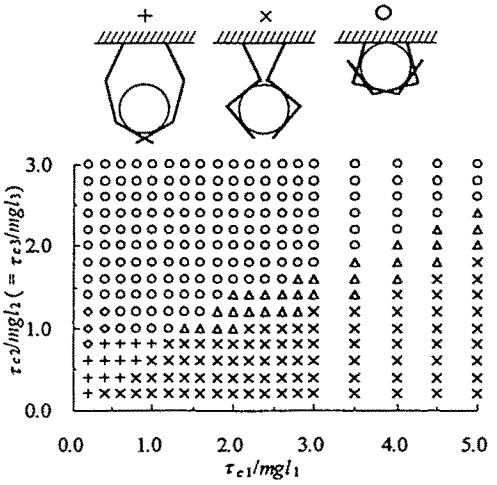

Fig.10 Map for judging the success or the failure (R=22.5[mm])

grasp, respectively. To avoid the complicated display, $\tau_{c3}=\tau_{c2}$ is imparted to the third joint. In the experiment, there are basically two failure modes. One is that the commanded torque are not big enough to finally lift up the object to the palm, where this case is shown by +. The other is that the command torque for the first joint is too big compared with that of the other joints and, as a result, the first link closes earlier than the remaining links envelop the object. The second case is shown by ×. In the second case, the object can not reach the palm. The second failure mode comes from the redundancy of the system, while it is more difficult for the two-link finger to have the similar configuration after two-points-contact mode. Of course, there are some ambiguous region between the success and the failure regions. This result is shown by △. From Fig.10, we would note that there exists a large number of combinations for achieving the target grasp. Through the whole experiments, the success rate was almost 100% for the object which can be enveloped by the hand.

7 Conclusions

We discussed the Scale-Dependent Enveloping Grasp based on the observation of human grasping and showed that human switches his (or her) grasp strategy according to the size of object, even though the object has a similar geometry. We also found that there are roughly three regions, the Direct-grasp, the Two-VFs-based transition grasp, and the Three-VFs-based transition grasp. Focusing on Two-VFs-based transition, we showed the determination of joint command torque for finally making the grasp object reach the palm. We confirmed that the proposed procedure works effectively by utilizing the Hiroshima Hand. Finally, we would like to express our sincere gratitude to Mr. N. Thaiprasert, Mr. Y. Hino, and Mr. Y. Tanaka for their cooperation for this work.

References

[1] Cutkosky, M.: On grasp choice, grasp models, and the design of hands for manufacturing tasks, *IEEE Trans. on Robotics and Automation*, vol.5, no.5, pp269–279, 1989.

[2] Bekey, G.A., H. Liu, R. Tomovic, and W. Karplus: Knowledge-based control of grasping in robot hands using heuristics from human motor skills, *IEEE Trans. on Robotics and Automation*, vol.9, no.6, pp709–722, 1993.

[3] Kang, S.B., and K. Ikeuchi: Toward automatic robot instruction from perception—Recognizing a grasp from observation, *IEEE Trans. on Robotics and Automation*, vol.9, no.4, pp432–443, 1993.

[4] Iberall, T., J. Jackson, L. Labbe, and R. Zampano: Knowledge-based pretension: Capturing human dexterity, *Proc. of the IEEE Int. Conf. on Robotics and Automation*, pp82–87, 1988.

[5] Stansfield, S.: Robotic grasping of unknown objects: A knowledge based approach, *Int. J. of Robotics Research*, vol.10, pp314–326, 1991.

[6] Jeannerod, M.: Attention and performance, chapter Intersegmental coordination during reaching at natural visual objects, pp153-168, Erlbaum, Hillsdale, 1981.

[7] Bard, C., and J. Troccaz: Automatic preshaping for a dexterous hand from a simple description of objects, *Proc. of the IEEE Int. Workshop on Intelligent Robots and Systems*, pp865-872, 1990.

[8] Kaneko, M., and K. Honkawa: Contact Point and Force Sensing for Inner Link Based Grasps, *Proc. of the IEEE Int. Conf. on Robotics and Automation*, pp2809-2814, 1994.

[9] Mirza, K., and D. E. Orin: Control of force distribution for power grasp in the DIGITS system, Proc. of the IEEE 29th CDC Conf., pp1960-1965, 1990.

[10] Trinkle, J. C., J. M. Abel, and R. P. Paul: Enveloping, frictionless planar grasping, *Proc. of the IEEE Int. Conf. on Robotics and Automation*, 1987.

[11] Salisbury, J. K., Whole-Arm manipulation, *Proc. of the 4th Int. Symp. of Robotics Research, Santa Cruz*, CA, 1987. Published by the MIT Press, Cambridge MA.

[12] Bicchi, A: Force distribution in multiple whole-limb manipulation, *Proc. of the IEEE Int. Conf. on Robotics and Automation*, pp196-201, 1993.

[13] Omata, T., and K. Nagata: Rigid body analysis of the indeterminate grasp force in power grasps, *Proc. of the IEEE Int. Conf. on Robotics and Automation*, pp1787-1794, 1996.

[14] Zhang, X-Y., Y. Nakamura, K. Goda, and K. Yoshimoto: Robustness of power grasp, *Proc. of the IEEE Int. Conf. on Robotics and Automation*, pp2828-2835, 1994.

[15] Kleinmann, K. P., J. Henning, C. Ruhm, and T. Tolle: Object manipulation by a multifingered gripper: On the transition from precision to power grasp, *Proc. of the IEEE Int. Conf. on Robotics and Automation*, pp2761-2766, 1996.

[16] Kaneko, M., Y. Tanaka, and T. Tsuji: Scale-dependent grasp, *Proc. of the IEEE Int. Conf. on Robotics and Automation*, pp2131-2136, 1996.